Bioinspired collagen–hydroxyethyl cellulose hydrogels for sustainable agriculture: Water management and plant growth stimulation

Laura Espindola-Serna
Universidad Rosario Castellanos
Melanie G. Franco-Martínez
Universidad Autónoma de Coahuila
María I. León-Campos
Universidad Autónoma de Coahuila
Juan J. Becerra-Rodríguez
Universidad Politécnica de Pénjamo
Denis A. Cabrera-Munguía
Universidad Autónoma de Coahuila
Dante A. López-Carmona
Universidad Autónoma de Chapingo, Estado de México
Martha Elena Domínguez-Hernández
Universidad Nacional Autónoma de México, Estado de México
Jesús A. Claudio-Rizo
jclaudio@uadec.edu.mx

Universidad Autónoma de Coahuila

Research Article

Keywords: Semi-interpenetrating polymer networks, Hydroxyethyl cellulose, Collagen-based hydrogels, Water retention, Plant cell adhesion and proliferation, Sustainable agriculture

Posted Date: July 11th, 2025

DOI: https://doi.org/10.21203/rs.3.rs-7032712/v1

Additional Declarations: No competing interests reported.

Version of Record: A version of this preprint was published at Journal of Polymers and the Environment on September 8th, 2025. See the published version at https://doi.org/10.1007/s10924-025-03675-5.

Abstract

The design of biodegradable hydrogels that enhance plant development while improving water management is gaining importance in sustainable agriculture. In this study, semi-interpenetrating polymer network (semi-IPN) hydrogels based on collagen and hydroxyethyl cellulose (HEC) were synthesized and evaluated for their physicochemical performance and plant cell interaction. Varying the HEC content (0–60 wt.%) modulated scaffold morphology, producing fibrillar-granular architectures with tunable gelation (3 min), superabsorbent capacity (>2800%), and thermal resistance. Increased HEC levels reduced chemical crosslinking (~27%) but improved mechanical stiffness (complex modulus up to 140 Pa), indicating strong physical interactions through hydrogen bonding. Biodegradability assays revealed rapid enzymatic degradation under collagenase exposure and slower hydrolytic and plant enzymatic breakdown, supporting scaffold stability during early plant development. When embedded in horticultural substrate, the hydrogels retained up to 92% of absorbed water and enabled gradual release over 15 days. Biological assays using tomato-derived plant cells (Solanum lycopersicum and Physalis philadelphica) confirmed that scaffolds with 20–40 wt.% HEC significantly enhanced cell adhesion, migration, metabolic activity, and proliferation. Seed germination studies in horticultural substrate further demonstrated that scaffolds containing 20 wt.% HEC promoted greater foliage development, while in vitro assays with MS-supplemented media revealed that C–HEC40% scaffolds effectively supported tomato growth through controlled sucrose delivery. These findings highlight collagen–HEC hydrogels as biodegradable, bioactive platforms with potential for moisture regulation, nutrient transport, and seedling support in environmentally responsible agricultural systems.

1.0 Introduction

Global agriculture is increasingly challenged by water scarcity, soil degradation, and an overreliance on agrochemicals, which collectively threaten food security and ecosystem health worldwide [1, 2]. Consequently, technologies that improve soil moisture retention and nutrient delivery while minimizing environmental impact are recognized as essential for advancing sustainable and resilient agri-food systems [3, 4]. Among these, hydrogels have emerged as cutting-edge materials due to their high water absorption capacity, biodegradability, and ability to enhance soil moisture dynamics [5–7]. Acting as efficient water reservoirs, hydrogels can release moisture gradually to crops, reducing irrigation frequency by up to 30% and minimizing water waste [3, 8, 9].

However, commercial synthetic hydrogels—such as those based on polyacrylates and polyacrylamide—despite their high absorption capacities, suffer from poor biodegradability and potential toxicity to soil biota, raising environmental concerns [10–12]. Additionally, their ability to actively stimulate plant metabolic activity remains limited, restricting their functionality as next-generation agricultural biomaterials [12, 13].

In contrast, hydrogels derived from natural polymers, including cellulose, chitosan, and lignin, are emerging as eco-friendly and multifunctional alternatives. These biopolymer-based hydrogels not only

retain and gradually release water but also facilitate controlled nutrient delivery and help reduce agricultural runoff [14–17]. Importantly, some biopolymer hydrogels are designed to mimic the structural and chemical functions of natural extracellular matrices, fostering beneficial interactions with plant cells. Such bioinspired materials have demonstrated potential in enhancing root proliferation, enzymatic activity, and overall plant vigor, contributing to improved crop productivity and soil health [18–20].

Although collagen hydrogels are traditionally used in biomedical applications, preliminary studies suggest their capacity to support plant cell adhesion, proliferation, and function—particularly in tomato-derived tissues [21–23]. This emerging evidence provides a strong rationale for exploring collagen-based hydrogels as novel agrobiomaterials.

Hydroxyethyl cellulose (HEC), a cellulose derivative known for forming hydrophilic networks with high swelling capacity, has been successfully employed to enhance soil moisture retention, improve aeration, and enable slow-release delivery of water and agrochemicals in horticultural substrates [24–26]. With growing regulatory and market demands for biodegradable and sustainable materials in agriculture, HEC-based hydrogels represent a promising platform for innovation [27, 28].

Motivated by these insights, we propose a novel semi-interpenetrating polymer network (semi-IPN) combining collagen and HEC. This hybrid system merges the bioactivity of collagen with the structural and water-management properties of HEC, creating a biodegradable scaffold that regulates moisture release and actively interacts with plant cells. We hypothesize that collagen–HEC semi-IPN hydrogels could serve as sustainable, bioinspired moisture-regulating matrices that also promote metabolic activity in plant cells, thereby enhancing tomato germination and growth. Therefore, the objective of this study is to synthesize and characterize collagen–HEC hydrogels with varying compositions, assess their physicochemical properties and biodegradation, and evaluate their effectiveness in supporting plant cell behavior—including adhesion, migration, and metabolism—as well as tomato seed germination and seedling development for sustainable agricultural applications.

2.0 Experimental section

2.1 Biopolymers and reagents

Porcine dermis was freshly obtained from a local butcher shop and processed for collagen extraction. HEC (M_w ~ 250 kDa), glycerol ethoxylate, hexamethylenediisocyanate, 2-propanol, ninhydrin, dextrose, sodium citrate, citric acid, sodium bicarbonate, magnesium chloride, calcium chloride, and Murashige and Skoog (MS) basal medium were purchased from *Sigma-Aldrich* (USA). Analytical-grade salts including sodium chloride, potassium chloride, monopotassium phosphate, sodium dihydrogen phosphate, and sodium hydroxide were obtained from *CTR Scientific* (Mexico).

2.2 Crosslinkers, dyes, and bioassay reagents

The MTT reagent [3-(4,5-dimethylthiazol-2-yl)-2,5-diphenyltetrazolium bromide] used for metabolic activity assays, as well as staining agents such as rhodamine B and ninhydrin, were supplied by *Sigma-Aldrich* (USA). All solutions were prepared using ultrapure water and analytical-grade reagents unless otherwise specified.

2.3 Plant material and substrate

Seeds of red tomato (*Solanum lycopersicum*) and green tomato (*Physalis philadelphica*) were provided by a certified local greenhouse. Commercial horticultural substrate (coconut fiber-based, enriched with compost and perlite) was purchased from the same supplier and used for degradation, germination and growth assays under controlled conditions.

2.4 Preparation and characterization of scaffolds

Type I collagen (M_w ~110–220 kDa) was extracted from porcine skin by enzymatic hydrolysis, following a previously reported protocol [29]. A polyurethane-based crosslinker was synthesized *via* the reaction of glycerol ethoxylate and hexamethylenediisocyanate, as described elsewhere (M_w ~3000–7500 Da) [30]. To reinforce the three-dimensional (3D) structure of the hydrogels, 15 wt.% of the synthesized polyurethane was incorporated into the collagen suspension (1 mg/mL) as a physical–chemical crosslinking agent [30]. Semi-IPN systems were generated by gradually adding HEC (1 wt.% solution) to the crosslinked collagen mixture at varying mass ratios. The pH of the resulting dispersion was carefully adjusted to 7.4 using 10× phosphate-buffered saline (PBS). The formulation was then poured into plates and incubated at 37°C for 24 hours to allow complete gelation and network stabilization. Table 1 summarizes the hydrogel formulations and the relative compositions of collagen, HEC, and crosslinker used in this study. HEC content was limited to a maximum of 60 wt.% in the formulations, as higher polysaccharide concentrations led to phase separation and compromised the structural homogeneity of the hydrogel network.

Table 1
Composition of collagen–HEC semi-IPN hydrogels used in this study.

Semi-IPN formulation	Type I collagen (mg)	Crosslinker (mg)	HEC (mg)
C	6	1.8	0
C-HEC20%	6	1.8	1.2
C-HEC40%	6	1.8	2.4
C-HEC60%	6	1.8	3.6

The structural and physicochemical properties of the hydrogels were assessed using multiple analytical techniques. Fourier transform infrared spectroscopy (FTIR) was performed using a *PerkinElmer* Frontier spectrometer to analyze functional group interactions. Wide-angle X-ray scattering (WAXS) patterns

were obtained with an *Anton-Paar* SAXS-Emc2 diffractometer to determine crystallinity. Microstructural morphology was visualized *via* scanning electron microscopy (SEM, *Jeol* JSM-7600F), and viscoelastic behavior was characterized using oscillatory rheometry (*Anton Paar* MCR 300). Swelling capacity was calculated as the ratio between the hydrated hydrogel mass and its corresponding dry mass. The degree of crosslinking was indirectly determined through ninhydrin assay. Additionally, gelation kinetics were monitored by turbidimetric measurements using a *ThermoScientific* MultiSkan Sky UV-Vis spectrophotometer.

Biodegradation behavior was assessed by monitoring mass loss of the hydrogels under different degradation conditions designed to simulate both biological and environmental scenarios relevant to their potential agricultural application. Proteolytic degradation was evaluated using collagenase (14 U/sample) and papain (14 U/sample), which represent key enzymatic mechanisms by which proteinaceous and polysaccharide components can be hydrolyzed. Collagenase was selected to simulate enzymatic activity from soil microorganisms capable of degrading collagen-based matrices [31], while papain—derived from *Carica papaya*—was used as a plant-derived protease representative of endogenous enzymatic activity in root environments and plant residues [32]. Additionally, hydrolytic degradation was evaluated using 1× PBS (pH 7.4) to simulate physiological-like aqueous environments that may be encountered in humid or irrigated soils [33]. Agricultural degradation was assessed by embedding the hydrogels in commercial vegetable substrate (10 g/gel) under ambient conditions to reflect a real-use scenario in horticultural systems [21, 23]. In all cases, the samples were analyzed for 15 days, and the percentage of mass loss was calculated relative to the initial weight to determine degradation.

To evaluate the ability of the hydrogels to gradually release water into the surrounding plant growth medium, a diffusion assay was performed using commercial vegetable substrate. For each experiment, pre-weighed hydrogel samples were placed in contact with 10 g of dry horticultural substrate within Petri dishes. A volume of 10 mL of distilled water was added daily to each setup to simulate regular irrigation under controlled conditions. After an initial swelling–diffusion equilibrium period of 1 hour at room temperature, the hydrogels were carefully removed and weighed. The amount of water diffused from the hydrogel into the substrate was calculated by comparing the change in hydrogel mass before and after contact, assuming negligible evaporation during the test period. The water released to the substrate (water diffusion (WD), expressed as a percentage) was determined using the following Eq. 1 (Eq. 1):

$$WD\ (\%) = \left(\frac{W_i - W_f}{W_i}\right) \times 100 \qquad \text{(Eq. 1)}$$

where, W_i is the initial mass of the fully swollen hydrogel before substrate contact, W_f is the final hydrogel mass after 1 hour of contact with the substrate. This method allowed indirect quantification of hydrogel-mediated water diffusion into the substrate, simulating field-relevant conditions of soil hydration over a 15-day period.

2.5 Biological evaluation: Plant cell behavior and seedling growth

To assess the biological response of plant systems to the developed hydrogels, different complementary assays were conducted. Tomato-derived cell cultures were established by isolating cells from seeds of red tomato (*Solanum lycopersicum*) and green tomato (*Physalis philadelphica*). The explants were cultured in MS medium under sterile conditions to obtain viable cell suspensions (1×10^5 cells/mL) [21, 23, 34]. The metabolic activity of cells exposed to different hydrogel formulations was evaluated using the MTT assay, based on the enzymatic reduction of the tetrazolium salt to formazan. Additionally, cell viability and proliferation were examined through fluorescence staining with rhodamine B reagent, allowing visualization of cell distribution and health in contact with the scaffolds [22, 23, 34].

To evaluate the interaction of plant cells with the hydrogel matrices, adhesion and migration assays were performed using cell cultures derived from both red tomato (*Solanum lycopersicum*) and green tomato (*Physalis philadelphica*). For each hydrogel formulation, 1 mL of cell suspension (1×10^5 cells/mL) was carefully seeded onto the surface of the hydrated hydrogels placed in sterile culture wells. The samples were incubated for 24 hours under sterile, humidified conditions at 25°C to allow cell attachment and migration into the hydrogel network. Following incubation, the hydrogels were gently rinsed with 1× PBS to remove non-adherent cells. Subsequently, the samples were fixed by immersion in glutaraldehyde (1 wt.%) for 10 minutes and then air-dried at room temperature. Cell adhesion and distribution were analyzed using an optical microscope equipped with phase-contrast. Images were captured to assess the extent of cell attachment and migratory penetration within the hydrogel structure, providing qualitative and quantitative data on cell–matrix interactions.

In other experiments, a plant growth assay was conducted to evaluate the functional effect of the scaffolds on tomato germination and early development. Red tomato seeds were embedded within the hydrogels and transferred to seedbeds filled with commercial horticultural substrate. The systems were maintained under controlled environmental conditions for 41 days, keeping the substrate moist by adding 30 mL of water every third day. Seedling growth was monitored periodically by recording morphological parameters, including the number of leaves and stem diameter. These data were used to analyze the relationship between hydrogel composition and plant development, providing insight into the stimulatory capacity of each matrix.

To evaluate the effect of the hydrogels on seed germination and early growth under controlled conditions, an *in vitro* germination assay was conducted. Agar gels supplemented with MS basal medium and sucrose (30 g/L) were prepared to simulate a nutrient-rich environment commonly used in plant tissue culture. This system served both as a control and support for hydrogel-based treatments. Surface-sterilized seeds of red tomato were placed directly on the MS–agar medium or on top of the scaffolds that were preconditioned in the same MS medium. All plates were incubated under sterile conditions at 25°C with a 16:8 h light/dark photoperiod. Seedling development was monitored over a 30-

day period. Parameters such as germination rate, number of leaves, root length, and stem diameter were recorded to assess the influence of the hydrogel formulations compared to the standard *in vitro* culture medium.

2.6 Statistical analysis

All experiments were performed in triplicate, and data are presented as mean values ± standard deviation (SD). Statistical differences among experimental groups were analyzed using one-way analysis of variance (ANOVA). When significant differences were detected, Tukey's post hoc test was applied to determine pairwise comparisons between group means. A confidence level of 95% was used to define statistical significance (* $p < 0.05$).

3.0 Results and discussion

3.1 Structural, morphological, and gelation characterization of collagen–HEC scaffolds

Collagen–HEC semi-IPN scaffolds exhibited a uniform appearance across all evaluated HEC concentrations, presenting a whitish-translucent coloration and excellent moldability. Notably, the hydrogels conformed precisely to the shape of the containers used during preparation (Fig. 1a), highlighting their adaptability to various formats. As HEC content increased, the overall volume of the hydrogel also expanded, indicating higher water uptake and network swelling. This tunable morphology and ease of handling are advantageous for agricultural applications, as the hydrogels can be shaped to fit seedbeds, root zones, or customized substrate compartments, facilitating integration into diverse cultivation systems [35].

SEM revealed that the scaffolds exhibit a characteristic fibrillar surface morphology typical of type I collagen-based hydrogels (Fig. 1b) [21, 22, 36]. In the semi-IPN systems, HEC granules were observed to be embedded within this fibrillar network. At 20 wt.% HEC (C-HEC20%), the granules appeared as small, well-dispersed clusters entangled among collagen fibers, maintaining the interconnected porosity seen in the collagen-only scaffold (C). As the HEC content increased, granule size also grew. In the C–HEC40% formulation, the overall fibrillar structure and porosity were largely preserved, though slightly less pronounced. However, in C–HEC60%, the extensive growth of HEC domains disrupted the collagen fiber alignment and reduced surface porosity.

These morphological changes are directly relevant to plant–material interactions. The fibrillar architecture with interconnected pores at lower to moderate HEC contents (20–40 wt.%) could facilitate water diffusion, nutrient transport, and potential root or cell penetration, all of which are critical for supporting seed germination and early plant development [37]. In contrast, the denser, less porous structure observed at higher HEC content (60 wt.%) could hinder mass transfer and reduce biological accessibility, limiting its suitability for sustainable agricultural applications [38]. Therefore, controlling the

polysaccharide content is key to optimizing scaffold architecture for effective soil moisture regulation and plant stimulation.

The effect of HEC content on the gelation capacity of the collagen-based hydrogels was investigated by monitoring turbidity changes through time-resolved absorbance measurements at 410 nm (Fig. 1c). This wavelength reflects the increase in light scattering associated with hydrogel network formation [22, 39]. The gelation kinetics of the systems showed a composition-dependent response. Formulations containing 20–40 wt.% HEC exhibited a characteristic three-phase gelation profile [39]. The first phase, marked by low and stable absorbance values, corresponds to a nucleation stage in which molecular interactions between the collagen fibrils and HEC chains initiate network formation through early physical–chemical crosslinking. This was followed by a second, linear phase with a pronounced increase in absorbance, indicating active assembly of the 3D hydrogel matrix as polymer–polymer interactions (including hydrogen bonding and physical entanglement) consolidate the semi-IPN structure. The final plateau phase, with stabilized high absorbance, reflects the completion of gelation, where residual rearrangements and secondary crosslinking events establish the final fibrillar morphology [36, 39]. In contrast, the formulation with 60 wt.% HEC deviated from this behavior. After approximately 40 minutes, a sharp decline in absorbance was observed, suggesting destabilization of the collagen fibrillar network. This phenomenon is attributed to steric and electrostatic repulsion between the collagen matrix and the oversized HEC aggregates, which disrupt the organized assembly of the gel and reduce crosslinking efficiency.

To further quantify gelation behavior, nucleation times were estimated from the onset of the turbidity curves (Fig. 1d). The collagen-only hydrogel (C) gelled in 16±1 min, while C–HEC20%, C–HEC40%, and C–HEC60% exhibited nucleation times of 19±2, 2±1, and 17±2 minutes, respectively. Notably, C–HEC40% displayed a significantly shorter nucleation time compared to all other systems, suggesting that at this intermediate concentration, HEC granules achieve an optimal size and dispersion that facilitates rapid physical crosslinking. This acceleration likely results from enhanced hydrogen bonding between HEC hydroxyl groups and polar functional groups in the collagen structure, reinforcing early-stage network formation.

From an agricultural perspective, rapid and efficient gelation is a critical attribute for hydrogel performance in seed coatings, nursery substrates, and *in situ* applications [5]. Faster gel formation supports practical deployment and mechanical integrity under irrigation [5, 37]. Moreover, optimized matrix structuring, as observed in C–HEC40%, could provide a favorable environment for plant cell adhesion and interaction. These properties are directly linked to improved seed germination, early root development, and sustained seedling vigor–key outcomes for sustainable agriculture and reduced dependence on external chemical inputs [37].

The interactions between functional groups within the semi-IPN hydrogels were elucidated by FTIR spectroscopy (Fig. 2). The spectrum of the collagen-based scaffold (C) exhibited characteristic stretching bands of hydroxyl (–OH) and amine (–NH) groups centered around 3400 cm^{-1}, corresponding

to abundant polar functionalities present in collagen amino acids (e.g., Gly, Pro, Hyp) and in the polyurethane crosslinker. Aliphatic –CH stretching vibrations were observed between 2800–2700 cm^{-1}, confirming the organic nature of the matrix. The typical amide I, II, and III vibration modes of collagen appeared at approximately 1650, 1560, and 1480 cm^{-1}, respectively, associated with C = O stretching, N–H bending, and C–N stretching within the polypeptide backbone.

A weak overtone at ~ 1730 cm^{-1}, attributed to urethane and urea linkages from the polyurethane network, indicates chemical crosslinking [30]. In-plane deformation bands corresponding to –NH and –CH vibrations were detected at ~ 1390 and 1260 cm^{-1}, while the C–O–C stretching vibrations of the flexible ether regions within the polyurethane structure appeared around 1100 cm^{-1} [30, 36, 39]. The FTIR spectra of the collagen–HEC semi-IPN scaffolds showed all the aforementioned functional groups; however, distinct changes were observed as HEC content increased. Specifically, the intensity of the broad –OH band at ~ 3400 cm^{-1}, the –CH deformation band at 1260 cm^{-1}, and the glycosidic C–O–C band at 1100 cm^{-1} progressively increased, reflecting the higher hydroxyl and carbohydrate content from HEC. Moreover, subtle yet consistent shifts in the wavenumbers of the amide I and II bands (highlighted in yellow in Fig. 2), as well as in the glycosidic region (highlighted in orange), were detected in HEC-containing systems. These spectral shifts suggest hydrogen bonding interactions between hydroxyl groups in HEC and polar regions of collagen, supporting the establishment of a physically interpenetrated network. Such hydrogen-bond-mediated crosslinks are central to the formation and stabilization of the semi-IPN architecture, contributing to the enhanced physical integrity and responsiveness of the hydrogel system [36, 39].

The inter- and intramolecular arrangements between collagen and HEC chains within the semi-IPN hydrogels were examined by WAXS analysis (Fig. 3). The collagen-only scaffold (C) exhibited sharp diffraction peaks at $2\theta \approx 32°$ and 46°, along with a weaker peak at 27.5°, indicating a high degree of molecular order and crystallinity. These peaks are associated with the well-aligned triple-helical structure and dense fibrillar packing characteristic of type I collagen [21, 22].

Upon incorporation of 20 wt.% HEC (C–HEC20%), the WAXS pattern changed notably. A broad amorphous halo centered around $2\theta \approx 22°$ emerged, corresponding to the granular, partially ordered nature of the polysaccharide [40]. Simultaneously, the intensity of the collagen diffraction peaks shifted: signals at 27.5° and 46° became more pronounced, while the peak at 32° decreased. This suggests that the inclusion of finely dispersed HEC granules within the fibrillar matrix perturbs the original collagen packing, as previously evidenced by SEM, leading to a semi-crystalline arrangement with modified interfibrillar spacing and local structural rearrangement.

In the C–HEC40% scaffold, the diffractogram exhibited stronger collagen-associated peaks at 27.5° and especially at 32°, while the amorphous HEC halo was no longer visible. This indicates a higher degree of fibrillar organization and densification of the collagen network, possibly due to favorable hydrogen bonding and entanglement at this HEC concentration. These interactions promote denser, more coherent fibrillar domains, as seen in SEM, and correlate with improved gelation behavior discussed earlier.

Conversely, the C–HEC60% scaffold presented a return to a semi-crystalline profile, with reappearance of the amorphous halo at ~ 22°, reflecting the dominant contribution of excess HEC. The intensity of the collagen peak at 32° diminished again, while signals at 27.5° and 46° increased. This suggests that large HEC aggregates disrupt the native collagen fibrillar organization, producing a more disordered interface, as supported by the SEM observations of disrupted surface porosity and altered fibril alignment. Overall, the WAXS analysis demonstrates that increasing HEC content progressively influences the molecular arrangement and crystallinity of collagen-based hydrogels. While intermediate HEC concentrations (20–40 wt.%) promote enhanced fibrillar ordering and network cohesion, higher HEC levels (60 wt.%) introduce more amorphous regions due to polysaccharide dominance. This suggests that physical entanglement and hydrogen bonding within the semi-IPN likely compensate for the reduction in crystallinity, contributing to the formation of stable matrices. Such structural features are promising for efficient moisture management and sustained plant cell interactions, key attributes for sustainable agricultural applications [22, 23, 41].

3.2 Physicochemical and mechanical characterization of bioinspired scaffolds

The swelling behavior of the scaffolds is presented in Fig. 4a, showing values of 1760±182%, 2372±195%, 2530±205%, and 2800±203% for C, C–HEC20%, C–HEC40%, and C–HEC60%, respectively. All formulations exhibited superabsorbent behavior –defined by water uptake exceeding 1000% of their dry weight– making them suitable candidates for moisture-regulating applications in agricultural substrates [5, 7]. A statistically significant increase was observed for the C–HEC60% hydrogel, highlighting the strong influence of HEC content on water absorption capacity.

This enhancement is attributed to the high concentration of hydrophilic –OH groups in the granular domains of HEC, physically entrapped within the collagen fibrillar network. SEM analysis supports this, revealing an increase in dispersed granular inclusions and variations in surface porosity at higher HEC concentrations, which facilitates greater water ingress.

Additionally, WAXS data showed that increasing HEC content introduces amorphous regions, which further enhances the hydration potential of scaffold. A high-water content prevents extensive collagen fibril aggregation, as previously observed in the gelation profiles, where excess HEC led to network destabilization and altered fibrillar assembly. This suggests that the semi-IPN collagen-HEC architecture can be precisely modulated to enhance water absorption efficiency. This is especially valuable for sustainable agriculture, where superabsorbent biomaterials contribute to efficient water management, reduced irrigation demands, and improved plant–soil interactions under limited water availability [1, 3, 14, 42].

The crosslinking degree of the scaffolds was evaluated by quantifying the free amino groups of collagen using the ninhydrin assay (Fig. 4b). Crosslinking indices of 42±4%, 39±5%, 24±4%, and 26±3% were obtained for C, C–HEC20%, C–HEC40%, and C–HEC60%, respectively. Significant differences were observed between the pure collagen-based matrices (C and C–HEC20%) and the hydrogels containing

higher HEC content (C–HEC40% and C–HEC60%), indicating that increasing the amount of polysaccharide results in a reduction in chemical crosslinking of collagen. This decrease can be attributed to the physical interference of HEC granules within the fibrillar collagen network. As revealed by FTIR (Fig. 2), the urea bond overtone associated with collagen–polyurethane crosslinking showed decreased intensity in the semi-IPN systems, reflecting reduced formation of covalent crosslinks. Larger HEC granules, especially in C–HEC60%, were seen to disrupt the native collagen fibril organization, further suggesting that steric repulsion and phase separation limit efficient molecular packing and chemical crosslinking.

Instead, the structural integrity of these hydrogels relies increasingly on physical crosslinking, primarily through hydrogen bonding between the abundant –OH groups in HEC and the polar groups of collagen. These interactions are particularly evident in C–HEC40%, which maintained a fibrillar architecture with good porosity and balanced swelling (Fig. 4a, 4c). This shift toward physically stabilized networks is advantageous in agricultural applications, where biodegradable and mechanically adaptable hydrogels are required to retain structure during water diffusion while still allowing gradual degradation and plant interaction [5, 14, 42].

Thermal stability of the collagen–HEC scaffolds was assessed via thermogravimetric analysis (TGA) (Fig. 5a).

The mass loss profiles revealed three distinct decomposition regions. The first, between 100–130°C, corresponds to surface water evaporation, showing ~ 4% mass loss across all formulations–indicative of physically absorbed water, consistent with the hydrophilic nature observed in swelling studies. The second region, spanning 200–450°C, is associated with the endothermic degradation of the polymeric components. Here, scaffolds C, C–HEC20%, and C–HEC40% showed mass losses around 76%, whereas C–HEC60% exhibited a lower loss (~ 63%), suggesting improved thermal stability. This effect is attributed to the higher density of physically crosslinked HEC domains, where abundant –OH groups establish extensive hydrogen bonding with collagen fibrils. As previously supported by FTIR and crosslinking index data, such interactions reinforce the matrix without relying on covalent crosslinking, thus delaying thermal degradation. The third region, observed between 600–800°C, represents the breakdown of residual polymer segments, leaving char residues between 10–19% for all samples. These residues likely reflect mineralized content and incomplete combustion of thermally stable regions such as hard polyurethane crosslinker segments.

DTGA analysis (Fig. 5b) provided further insight into the thermal behavior of individual components. The peak at ~ 86°C corresponds to water loss retained within the matrix, possibly stabilized by interstitial repulsion between HEC granules and collagen fibrils. Collagen degradation peaks appeared between 220–250°C, shifting slightly upward with increasing HEC content. This indicates that hydrogen bonding between HEC and collagen increases the thermal energy required to initiate degradation, a stabilizing effect consistent with enhanced fibrillar arrangement observed by WAXS in C–HEC40%. HEC granule degradation occurred between 350–425°C, with C–HEC20% showing a higher decomposition

temperature, likely due to smaller, more dispersed granules that integrate better with the collagen network and resist early breakdown. Polyurethane hard segment degradation appeared around 470°C in all formulations, confirming structural contributions from the crosslinker.

Altogether, the semi-IPN structure –especially at intermediate HEC concentrations–yields scaffolds with enhanced thermal resilience, an advantageous property in agricultural environments where temperature fluctuations, microbial activity, and biodegradation coexist [5, 7, 14]. Thermal stability ensures that the hydrogel can maintain its moisture-regulating and structural functions long enough to support germination and early seedling development before controlled degradation occurs [14].

The viscoelastic behavior of the collagen–HEC hydrogels was evaluated to understand their mechanical stability under hydrated conditions (Fig. 5c). All scaffolds exhibited a typical hydrogel-like profile, where the storage modulus (G') surpassed the loss modulus (G") (G'>G"), indicating a predominantly elastic response across the frequency range. At a fixed oscillation frequency of 1 Hz, G' values of 20 Pa, 23 Pa, 35 Pa, and 100 Pa were recorded for C, C–HEC20%, C–HEC40%, and C–HEC60%, respectively. The significant increase in G' for C–HEC60% suggests that higher HEC content notably enhances the resistance of the matrix to deformation. This reinforcement is attributed to the physical crosslinking *via* hydrogen bonding between the hydroxyl-rich HEC granules and the collagen fibrillar network. Larger HEC domains become embedded within the matrix, improving the compactness and cohesion of the scaffold. Despite reduced crystallinity at high HEC levels, the semi-IPN structure remains mechanically robust due to physical entanglement. TGA results also confirmed this mechanical stability, showing delayed thermal degradation in highly crosslinked systems.

Frequency sweep analysis showed that the complex modulus (G*) increased steadily between 0.1–100 Hz for all formulations, with C–HEC60% maintaining the highest G* (~ 100 Pa) throughout the frequency range. This rheological profile indicates that the scaffold remains structurally stable under dynamic stress, a key factor in resisting mechanical disturbances in soil or plant beds [5, 43]. These mechanical properties are highly relevant for agricultural applications, particularly in the encapsulation of seeds, *in situ* cell growth, and early-stage plant support [21–23]. Hydrogels with tunable elasticity and strength ensure proper contact with seeds and roots, protect against physical stress, and maintain structural coherence during water retention and diffusion [21, 23]. Moreover, mechanically resilient scaffolds prevent premature collapse, enabling consistent metabolic stimulation and germination support over extended periods [14, 22].

3.3 Scaffold performance for agricultural applications: Biodegradation and water diffusion in horticultural substrate

Biodegradation assays were conducted under three distinct conditions to evaluate the environmental responsiveness of the collagen–HEC semi-IPN scaffolds. As shown in Fig. 6a, under collagenase exposure, all scaffolds—regardless of HEC content—underwent complete mass loss (100%) within the

incubation period. This confirms a high susceptibility to proteolytic degradation, indicating that microbial enzymes naturally present in agricultural soils can efficiently degrade these scaffolds. Notably, the presence of HEC granules and variations in collagen crystallinity did not hinder collagenase activity. This suggests that although HEC modifies the fibrillar architecture, it does not sterically block enzymatic access to peptide bonds within the collagen backbone.

In contrast, degradation in papain-containing medium was considerably slower, with all matrices showing only ~ 9% mass loss after incubation. No significant differences were observed across the formulations, suggesting that the polyurethane-crosslinked collagen network resists hydrolysis by plant-derived cysteine proteases. The absence of correlation with HEC content indicates that the granular architecture does not facilitate or hinder papain access, pointing to the protective effect of polyurethane-mediated crosslinking and dense fibrillar networks.

Under hydrolytic conditions in PBS, the scaffolds exhibited moderate degradation. Scaffolds C and C–HEC20% lost approximately 10% of their mass, while C–HEC40% and C–HEC60% displayed significantly higher degradation (~ 20%). This increase aligns with the larger HEC granules occluded in the fibrillar matrix. These granules likely swell and disrupt fibrillar cohesion over time, making the matrix more prone to hydrolytic disassembly. This trend also correlates with lower chemical crosslinking (Fig. 4b) and enhanced swelling (Fig. 4a), indicating that the predominance of physical crosslinks (e.g., hydrogen bonding) leads to increased water sensitivity.

These biodegradation profiles suggest tunability: while all scaffolds are rapidly degradable under microbial enzymatic conditions —desirable for minimizing long-term soil residues— their slower degradation under hydrolytic and plant enzymatic conditions ensures structural integrity during early plant development [14, 21, 23]. This balance is crucial for controlled matrix persistence, water retention, and nutrient delivery, making the collagen–HEC scaffolds promising candidates for eco-compatible, degradable agrobiomaterials in sustainable agriculture [3, 5, 6, 43].

The degradation profile of the scaffolds in contact with a commercial horticultural substrate — composed primarily of peat moss, coconut coir, vermiculite, and slow-release fertilizers— was assessed over time (Fig. 6b). Upon initial exposure, all hydrogels experienced a rapid mass loss of approximately 92–95% within the first 24 hours, which is attributed not to scaffold degradation but to water diffusion from the hydrogel to the surrounding substrate. This substantial water transfer aligns with the superabsorbent nature of the materials (swelling > 2000%, Fig. 4a) and confirms their capacity to act as moisture reservoirs that release water gradually into dry soils [3, 10, 21, 24]. After this initial dehydration phase, no further mass loss was detected over the following days, with scaffolds stabilizing as xerogels with residual masses between 5–8%, depending on composition. Importantly, the mass retention increased with higher HEC content. Scaffolds containing 40–60 wt.% HEC retained more mass after water release, which correlates with the presence of robust HEC granules entrapped in the fibrillar collagen matrix.

These findings also reflect the thermal stability and reduced chemical crosslinking of high-HEC formulations, which favor physical entanglement and hydrogen bonding over irreversible chemical bonding. The fibrillar disruption and amorphous contributions of HEC (Fig. 3) appear to allow the structure to remain intact post-hydration without rapid breakdown, suggesting a reversible hydration–dehydration behavior ideal for multiple irrigation–drying cycles in horticultural settings [25, 27, 41].

From an agricultural application standpoint, this behavior is highly beneficial: the scaffold releases its water load effectively into the plant root zone but remains physically present to maintain root contact, avoid soil compaction, and potentially interact with root-secreted enzymes or metabolites [5, 14, 21]. Moreover, the progressive increase in mechanical strength (Fig. 5c) with increasing HEC supports structural resilience during handling and implantation [23, 24, 35, 42]. Interestingly, these results indicate that collagen–HEC hydrogels are not degraded by the components of the commercial substrate, making them chemically stable yet highly functional under horticultural conditions. This stability enables their use as bioinspired seed or root coatings, plant cell scaffolds, or soil conditioners that deliver moisture while maintaining contact with plant tissues during early stages of development—a key asset for improving germination rates, reducing water stress, and promoting sustainable agriculture [6, 21, 23].

To simulate field-relevant water release behavior, water diffusion from swollen collagen–HEC scaffolds into a commercial vegetable substrate was evaluated over 15 days (Fig. 6c). On day 1, all scaffolds released a substantial portion of their absorbed water, transferring between 80–88% of their moisture load into the substrate. Hydrogels with 40 and 60 wt.% HEC exhibited the highest release, consistent with their enhanced swelling capacity (Fig. 4a) and fibrillar–granular architecture that facilitates gradual moisture flow (Fig. 1b, SEM). Over the 15-day period, all hydrogels maintained a stable water diffusion profile, culminating in total transfer values of 81%, 83%, 90%, and 93% for C, C-HEC20%, C-HEC40%, and C-HEC60%, respectively. These results highlight the importance of HEC content in modulating water delivery. The granular domains formed by HEC create hydrophilic channels within the collagen matrix, which support sustained moisture release through capillary and diffusion-driven mechanisms [3, 21, 23]. From a sustainability perspective, this gradual and consistent water release is ideal for reducing irrigation frequency, minimizing water waste, and alleviating drought stress during germination and early seedling development [3, 5, 14, 28]. Unlike conventional superabsorbent polymers, which may swell excessively and then rapidly dehydrate [12, 44], these bioinspired semi-IPN scaffolds act as smart reservoirs, releasing moisture in a controlled manner while maintaining mechanical resilience and structural stability in the soil environment. Therefore, collagen–HEC hydrogels—particularly those with 40–60 wt.% HEC—represent a promising biodegradable alternative to synthetic water-retention agents in agriculture, with a performance profile tailored to support seed germination, root establishment, and sustainable crop growth in resource-limited conditions [6, 10, 24].

3.4 Scaffold–Plant cell interactions: Adhesion, migration, and metabolism

Tomato-derived plant cells obtained from red tomato (*Solanum lycopersicum*) and green tomato (*Physalis philadelphica*) seeds were used to investigate the interaction between plant cells and the hydrogel scaffolds, offering insights into their bioactivity for agricultural applications. The adhesion and migration patterns of these cells growing in contact with the biomatrices (Fig. 7a) reveal that the fibrillar–granular hybrid architecture of the semi-IPN scaffolds effectively supports both cellular functions.

The morphology of the scaffolds shows that C-HEC20% and C-HEC40% scaffolds exhibit finely dispersed HEC granules embedded within an interconnected fibrillar collagen network. This configuration appears to facilitate surface adhesion and inward migration of plant cells, as indicated by dense cellular coverage and the presence of internalized cells at scaffold interfaces.

These systems, which also demonstrated enhanced swelling capacity and moderate viscoelastic resistance, provide a hydrated and mechanically compliant microenvironment that mimics natural plant extracellular conditions, thus promoting cell infiltration [20, 22]. In contrast, the scaffold without HEC (C) also supports notable adhesion and cell migration, likely attributed to its highly ordered fibrillar structure. However, the lower swelling capacity and denser network may limit deeper cell infiltration compared to C-HEC20% and C-HEC40%, where the fibrillar–granular architecture offers a more permissive and hydrated environment for cellular migration. On the other end, the C-HEC60% matrix, despite having the highest swelling and stiffness values (highest G*), shows reduced cellular confluence and hindered migration, likely due to the excessive surface granulation and decreased porosity from HEC aggregation, which may act as physical barriers to cellular penetration.

These results indicate that an intermediate HEC content (20–40 wt.%) achieves an optimal balance between scaffold hydration, structural flexibility, and biochemical compatibility—key parameters that support plant cell adhesion, migration, and metabolic activation [21, 23]. Such features are highly desirable for applications in seed encapsulation, germination matrices, and root-zone plant interfaces, where controlled water management and bioactivity can synergistically enhance early plant development [14, 20]. This highlights the potential of collagen–HEC scaffolds as bioinspired platforms for sustainable agriculture, supporting both physical water regulation and active biological stimulation.

The metabolic activity of red tomato (*Solanum lycopersicum*) cells cultured on the scaffolds was evaluated using the MTT assay (Fig. 7b). After 24 hours of contact, significant metabolic stimulation was observed for all scaffold systems compared to the control (100%), with relative activity levels of 192 ± 13% (C), 204 ± 16% (C-HEC20%), 162 ± 11% (C-HEC40%), and 145 ± 10% (C-HEC60%). These results confirm that none of the scaffolds exert cytotoxic effects on plant cells and, conversely, enhance their metabolic functions. At 48 hours, metabolic activity further increased across all scaffolds, with the highest value recorded for the collagen-only matrix (C, 348 ± 28%), likely due to the abundance of bioactive amino acid residues and its dense fibrillar architecture that actively supports cell viability and function [21, 23]. Interestingly, scaffolds containing 20 and 40 wt.% HEC also sustained significant stimulation (290–310%), outperforming the 60 wt.% formulation. This behavior correlates with previous

findings from SEM and adhesion/migration assays, where C-HEC20% and C-HEC40% provided optimal fibrillar–granular interfaces and swelling capacity, promoting effective cell–matrix interactions. In contrast, the C-HEC60% scaffold, despite its high-water content, showed lower metabolic activation. This could be attributed to excessive granulation of HEC interfering with effective cell adherence and migration, thereby limiting intimate contact with metabolically active collagen domains.

In the case of green tomato (*Physalis philadelphica*) cells (Fig. 7c), all scaffold formulations promoted metabolic activity above the control level (100%) after 24 h of incubation, confirming the non-cytotoxic nature of the scaffolds toward this cell type. Metabolic activity values were 245 ± 19% (C), 182 ± 16% (C-HEC20%), 162 ± 12% (C-HEC40%), and 261 ± 20% (C-HEC60%). Notably, scaffolds C and C-HEC60% showed significantly higher stimulation compared to the intermediate formulations, suggesting two distinct yet effective mechanisms of action. For scaffold C, the strong early metabolic stimulation is likely attributed to its dense fibrillar collagen network rich in amino acids such as glycine, proline, and hydroxyproline—known to support cellular signaling and growth [21, 23, 45]. Meanwhile, the C-HEC60% scaffold, despite its more amorphous microstructure, likely benefits from high water content and larger HEC granules, which facilitate rapid swelling and diffusional transport of water and soluble bioactive degradation byproducts (e.g., saccharide units from HEC and peptides from collagen), which can be metabolized by plant cells as nutrient sources [24, 27, 46].

After 48 h of culture, a general decline in metabolic activity was observed across all scaffolds, though values remained above 100%, indicating sustained metabolic support after initial adaptation. Interestingly, at this later time point, the highest activity was recorded in scaffolds with 20 and 40 wt.% HEC content, which showed significant differences compared to C and C-HEC60%. This delayed metabolic stimulation can be explained by the optimal balance of fibrillar and granular architecture in C-HEC20% and C-HEC40%, which promotes stable cell adhesion, migration, and gradual release of degradation products, supporting prolonged interaction with plant cells. Swelling and mechanical analyses showed these formulations possess moderate elasticity and water retention, allowing sustained hydration and scaffold integrity. Biodegradation studies indicated that controlled release of bioactive components occurs in these systems under both enzymatic and substrate-mimicking conditions, stimulating the plant cell metabolism. These insights highlight the versatility of semi-IPN collagen–HEC scaffolds in modulating plant cell responses, offering a promising platform for the development of bioactive agricultural biomatrices tailored to specific crop types and developmental stages [5, 16, 20].

The proliferative capacity of tomato-derived cells in contact with the scaffolds was also investigated using epifluorescence microscopy with the vital dye rhodamine B to identify metabolically active living cells (Fig. 7d). Intense red fluorescent zones—indicative of active cell proliferation—were observed in all scaffold formulations for both red and green tomato cell types, confirming that the bioinspired semi-IPN scaffold not only supports cell adhesion and migration but also promotes cell division and sustained metabolic function.

This widespread cellular proliferation correlates with the earlier MTT assay results, reinforcing that the scaffolds do not exert cytotoxic effects and instead foster a biologically favorable microenvironment. The presence of both bioactive amino acids of collagen and the hydrophilic character of HEC facilitates water availability and diffusion of small molecules, which can be utilized by the cells as nutrients or signaling cues [16, 23, 24]. Scaffolds containing 20 and 40wt.% HEC (C-HEC20% and C-HEC40%) displayed the most extensive proliferative zones, with densely populated and evenly distributed fluorescent areas.

In contrast, the C-HEC60% scaffold exhibited noticeably fewer fluorescent proliferative regions, suggesting that excessive HEC content may hinder optimal cell–matrix interactions. As previously discussed, this formulation's larger HEC granules disrupt collagen fibril organization and increase stiffness, possibly creating a less favorable microenvironment for cell spreading and division. Moreover, the rapid initial swelling of this matrix may lead to faster loss of water and soluble factors, reducing long-term support for cell proliferation [47, 48].

These results demonstrate that scaffold composition—especially the balance between fibrillar collagen and granular HEC—directly influences not only cell adhesion and metabolism but also the ability of plant-derived cells to proliferate within the matrix. This capacity is essential for developing smart biomaterials aimed at stimulating plant tissue regeneration, enhancing seedling vigor, or delivering bioactive cues in sustainable agriculture [10, 21, 38].

3.5 Tomato seed germination performance on collagen–HEC scaffolds

Red tomato seed germination and early plant development were evaluated over 41 days using a commercial horticultural substrate (Fig. 8a). Only the C-HEC20% and C-HEC40% scaffolds were tested, as these formulations previously demonstrated the most favorable biological interactions with tomato-derived plant cells. Growth performance was compared to a control group in which seeds were germinated directly in substrate without hydrogels.

Stem length measurements after 41 days revealed no statistically significant differences among the groups, with all treatments reaching an average height of ~ 8 cm (Fig. 8b). Similarly, stem diameters remained consistent at around 2.3 mm across all conditions (Fig. 8c), indicating that the scaffolds did not negatively impact structural stem development. In contrast, significant differences were observed in leaf number—an important indicator of photosynthetic surface area and early vigor [14, 21, 38, 49]. Control plants developed an average of 5 leaves, whereas plants grown on C-HEC20% and C-HEC40% scaffolds produced 9 and 8 leaves, respectively.

The increased foliar development in the C-HEC20% group was statistically significant, suggesting that the microarchitecture and water-management capacity of this scaffold enhanced morphogenetic processes involved in leaf emergence. These findings support the notion that scaffold-assisted germination—particularly with the C-HEC20% formulation—can enhance early shoot development, likely

due to optimal water retention, mechanical compliance, and bioactive signaling from collagen and HEC degradation byproducts. From an agricultural perspective, such bioinspired hydrogel systems offer a sustainable platform for improving seedling establishment and early crop vigor, especially under conditions of limited irrigation or suboptimal substrates [5, 10, 21, 24].

To further assess the potential of the scaffolds in supporting seed germination under defined nutrient conditions, *in vitro* assays were conducted using agar supplemented with MS medium, with and without sucrose (Fig. 8e). As expected, MS(+) promoted robust seedling development due to the availability of an accessible carbon source [50]. Remarkably, when combined with the C-HEC40% scaffold, plant growth was significantly enhanced, with observable improvements in stem thickness, leaf number, and overall vigor. This result suggests that the C-HEC40% hydrogel matrix not only provides mechanical and hydration support but also acts as an effective carrier and slow-release platform for nutrients like sucrose. Its high swelling capacity and semi-interpenetrating architecture facilitate the gradual diffusion of nutrients into the surrounding medium, thereby sustaining early plant metabolism [5, 11]. This controlled delivery effect becomes especially evident in the enhanced plant development observed under sucrose-enriched conditions.

Although no significant stimulation was observed in the absence of sucrose, this highlights the role of scaffold as a nutrient-responsive system capable of delivering incorporated bioactive molecules. These findings underscore the potential of collagen–HEC hydrogels as customizable platforms for encapsulating and gradually releasing not only carbon sources but also other agro-inputs (e.g., biostimulants, micronutrients, phytohormones), thereby offering a smart and sustainable strategy for improving seed germination and early plant growth [5, 6, 11, 14, 23].

4.0 Conclusions

This study demonstrates that bioinspired collagen–HEC semi-IPN hydrogels possess tunable physicochemical and biological properties suitable for sustainable agricultural applications. By varying the HEC content, we were able to modulate scaffold crystallinity, microstructure, water absorption, mechanical behavior, and degradation profiles—key parameters for optimizing soil–plant interactions. Hydrogels containing 20–40 wt.% HEC exhibited optimal performance, combining high water retention capacity, structural integrity, and compatibility with tomato-derived plant cells. These formulations promoted cell adhesion, migration, and metabolic activity without cytotoxic effects, and notably enhanced seedling foliage during germination. Furthermore, C-HEC40% scaffolds showed promising behavior as sucrose delivery systems under *in vitro* conditions, suggesting their potential as carriers for nutrients or biostimulants. Altogether, the results position collagen–HEC hydrogels as multifunctional bioactive scaffolds that mimic natural plant–soil interfaces, offering a promising strategy for controlled hydration, cell support, and growth stimulation in modern sustainable agriculture.

Declarations

Author contributions statement

All authors read and approved the final manuscript.

Conflict of interest

The author declare that they have no competing interest.

Contributions

Laura Espindola-Serna, Melanie G. Franco-Martínez: Writing – original draft, Formal analysis, Data curation, Conceptualization. Jesús A. Claudio-Rizo: Writing – review & editing, Writing – original draft, Visualization, Validation, Supervision, Software, Resources, Project administration, Methodology, Investigation, Funding acquisition, Formal analysis, Data curation, Conceptualization. Maria I. León-Campos: Writing – review & editing, Validation, Methodology, Formal analysis. Juan J. Becerra-Rodríguez: Writing – review & editing, Methodology, Formal analysis. Denis A. Cabrera-Munguía: Writing – review & editing, Methodology, Formal analysis. Dante A. López-Carmona: Writing – review & editing, Supervision, Methodology. Martha Elena Domínguez-Hernández: Writing – review & editing, Supervision, Methodology.

Acknowledgements

The authors thank the Secretaría de Ciencia, Humanidades, Tecnología e Innovación (SECIHTI) for supporting the FORDECYT-PRONACES/6660/2020 project, and to Jesús Alfonso Mercado Silva for technical support in DRX and TGA studies.

Data availability

Data will be made available upon reasonable request.

References

1. G.M. Robinson, Global sustainable agriculture and land management systems, Geography and Sustainability 5(4) (2024) 637-646.
2. T. Gomiero, Soil Degradation, Land Scarcity and Food Security: Reviewing a Complex Challenge, Sustainability, 2016.
3. Y. Oladosu, M.Y. Rafii, F. Arolu, S.C. Chukwu, M.A. Salisu, I.K. Fagbohun, T.K. Muftaudeen, S. Swaray, B.S. Haliru, Superabsorbent Polymer Hydrogels for Sustainable Agriculture: A Review, Horticulturae, 2022.

4. A.F. Chamorro, M. Palencia, E.M. Combatt, Starch Hydrogels for Slow and Controlled-Release Fertilizers: A Review, Polymers, 2025.
5. K. Ali, Z. Asad, G.H.D. Agbna, A. Saud, A. Khan, S.J. Zaidi, Progress and Innovations in Hydrogels for Sustainable Agriculture, Agronomy, 2024.
6. P. Kaur, R. Agrawal, F.M. Pfeffer, R. Williams, H.B. Bohidar, Hydrogels in Agriculture: Prospects and Challenges, Journal of Polymers and the Environment 31(9) (2023) 3701-3718.
7. J. Park, W. Guan, G. Yu, Smart Hydrogels for Sustainable Agriculture, EcoMat 7(4) (2025) e70011.
8. J. Park, W. Guan, C. Lei, G. Yu, Self-Irrigation and Slow-Release Fertilizer Hydrogels for Sustainable Agriculture, ACS Materials Letters 6(8) (2024) 3471-3477.
9. S.S. Rathore, K. Shekhawat, S. Babu, V.K. Singh, Mitigating moisture stress in Brassica juncea through deficit irrigation scheduling and hydrogel in ustocherpts soils of semi-arid India, Heliyon 6(12) (2020) e05786.
10. I. Piccoli, C. Camarotto, A. Squartini, M. Longo, S. Gross, M. Maggini, M.L. Cabrera, F. Morari, Hydrogels for agronomical application: from soil characteristics to crop growth: a review, Agronomy for Sustainable Development 44(2) (2024) 22.
11. S.K. Patra, R. Poddar, M. Brestic, P.U. Acharjee, P. Bhattacharya, S. Sengupta, P. Pal, N. Bam, B. Biswas, V. Barek, P. Ondrisik, M. Skalicky, A. Hossain, Prospects of Hydrogels in Agriculture for Enhancing Crop and Water Productivity under Water Deficit Condition, International Journal of Polymer Science 2022(1) (2022) 4914836.
12. Y.C. Cheng, C.P. Wang, K.Y. Liu, S.Y. Pan, Towards sustainable management of polyacrylamide in soil-water environment: Occurrence, degradation, and risk, The Science of the total environment 926 (2024) 171587.
13. K. Tabra, E.C. Arellano, S. Contreras, R. Ginocchio, Evaluation of phytotoxic effects of cationic polyacrylamide polymers: implication for the use of sludges as organic soil amendments in assisted phytostabilization, International journal of phytoremediation 22(10) (2020) 1068-1074.
14. D.N. Iqbal, Z. Tariq, B. Philips, A. Sadiqa, M. Ahmad, K.M. Al-Ahmary, I. Ali, M. Ahmed, Nanocellulose/wood ash-reinforced starch-chitosan hydrogel composites for soil conditioning and their impact on pea plant growth, 14(13) (2024) 8652-8664.
15. P. Laddawan, S. Auecharoenrat, C. Tongsook, Environmentally Friendly Carboxymethyl Cellulose Hydrogels Derived from Waste Paper and Sawdust as a Urea Release Agent, ACS Omega 10(17) (2025) 17296-17309.
16. Z. Tariq, D.N. Iqbal, Significance of biopolymer-based hydrogels and their applications in agriculture: a review in perspective of synthesis and their degree of swelling for water holding, 13(35) (2023) 24731-24754.
17. P. Lee, X. Lin, F. Khan, A.E. Bennett, J.O. Winter, Translating controlled release systems from biomedicine to agriculture, Frontiers in Biomaterials Science Volume 1 - 2022 (2022).
18. H. Geckil, F. Xu, X. Zhang, S. Moon, U. Demirci, Engineering hydrogels as extracellular matrix mimics, Nanomedicine (London, England) 5(3) (2010) 469-84.

19. J.Y. Ng, S. Obuobi, M.L. Chua, C. Zhang, S. Hong, Y. Kumar, R. Gokhale, P.L.R. Ee, Biomimicry of microbial polysaccharide hydrogels for tissue engineering and regenerative medicine – A review, Carbohydrate Polymers 241 (2020) 116345.
20. R. Calcutt, R. Vincent, D. Dean, Plant cell adhesion and growth on artificial fibrous scaffolds as an in vitro model for plant development, 7(43) (2021) eabj1469.
21. V.G. Oyervides-Guajardo, J.A. Claudio-Rizo, D.A. Cabrera-Munguía, M. Caldera-Villalobos, T.E. Flores-Guia, F. Soriano-Corral, A. Herrera-Guerrero, BioZnMOFs dispersed in collagen-starch hydrogels: a stimulating approach for animal and plant tissue growth, Macromolecular Research 32(11) (2024) 1097-1112.
22. M.P. Flores-Urquieta, C.-R.J. A., C.-M.D. A., C.-S.L. F., F.-G.T. E., E.-N. Roberto, J.J. and Becerra-Rodriguez, Studying the impact of selenium complex chemical structure on collagen-starch hydrogels for enhanced tissue growth, Soft Materials 22(4) (2024) 325-341.
23. C.I. Valdés-Lozano, J.A. Claudio-Rizo, D.A. Cabrera-Munguía, M.I. León-Campos, J.J. Mendoza-Villafaña, J.J. Becerra-Rodriguez, Modulation of animal and plant tissue growth with collagen-starch-organic molybdenum networks hydrogel biomatrices, Polymers for Advanced Technologies 35(9) (2024) e6568.
24. N. Ranganathan, R. Joseph Bensingh, M. Abdul Kader, S.K. Nayak, Cellulose-Based Hydrogels for Agricultures, in: M.I.H. Mondal (Ed.), Cellulose-Based Superabsorbent Hydrogels, Springer International Publishing, Cham, 2018, pp. 1-21.
25. A. Noreen, K.M. Zia, S. Tabasum, S. Khalid, R. Shareef, A review on grafting of hydroxyethylcellulose for versatile applications, International journal of biological macromolecules 150 (2020) 289-303.
26. Y. Seki, A. Altinisik, B. Demircioğlu, C. Tetik, Carboxymethylcellulose (CMC)–hydroxyethylcellulose (HEC) based hydrogels: synthesis and characterization, Cellulose 21(3) (2014) 1689-1698.
27. C. Chang, L. Zhang, Cellulose-based hydrogels: Present status and application prospects, Carbohydrate Polymers 84(1) (2011) 40-53.
28. H. Omidian, A. Akhzarmehr, S.D. Chowdhury, Advancements in Cellulose-Based Superabsorbent Hydrogels: Sustainable Solutions across Industries, Gels (Basel, Switzerland), 2024.
29. J.A. Claudio-Rizo, M. Rangel-Argote, L.E. Castellano, J. Delgado, J.L. Mata-Mata, B. Mendoza-Novelo, Influence of residual composition on the structure and properties of extracellular matrix derived hydrogels, Materials science & engineering. C, Materials for biological applications 79 (2017) 793-801.
30. M. Caldera-Villalobos, D.G. Ramos-Montañez, D.A. Cabrera-Munguía, J.J. Becerra-Rodriguez, N. Rodríguez-Fuentes, J.A. Claudio-Rizo, Biocompatible hydrogels comprised of collagen, chitosan and polyurethane with potential applications for wound healing and controlled drug release, Polymer International 74(1) (2025) 9-19.
31. L.A. Lima, R.F. Cruz Filho, J.G. dos Santos, W.C. Silva, Protease with collagenolytic activity produced by Bacillus sp. DPUA 1728 from Amazonian soil, Brazilian journal of microbiology : [publication of the Brazilian Society for Microbiology] 46(4) (2015) 1217-23.

32. T. Shindo, R.A. Van der Hoorn, Papain-like cysteine proteases: key players at molecular battlefields employed by both plants and their invaders, Molecular plant pathology 9(1) (2008) 119-25.
33. D. Neina, The Role of Soil pH in Plant Nutrition and Soil Remediation, Applied and Environmental Soil Science 2019(1) (2019) 5794869.
34. L.K. Usme-Duque, J.A. Claudio-Rizo, J.A. Nuncio-Esquivel, M.I. León-Campos, M. Cruz-Requena, L.J. Ríos-González, J.A. Ascacio- Valdés, M.A. Medina-Morales, Optimization of fungal fermentation for the extraction of polyphenols from Flourensia cernua and its effect on cellular metabolism, Journal of Biotechnology 401 (2025) 60-73.
35. Z. Tariq, D.N. Iqbal, M. Rizwan, M. Ahmad, M. Faheem, M. Ahmed, Significance of biopolymer-based hydrogels and their applications in agriculture: a review in perspective of synthesis and their degree of swelling for water holding, RSC Advances 13(35) (2023) 24731-24754.
36. E.E. Lopéz-Martínez, J.A. Claudio-Rizo, M. Caldera-Villalobos, J.J. Becerra-Rodríguez, D.A. Cabrera-Munguía, L.F. Cano-Salazar, R. Betancourt-Galindo, Hydrogels for Biomedicine Based on Semi-Interpenetrating Polymeric Networks of Collagen/Guar Gum: Synthesis and Physicochemical Characterization, Macromolecular Research 30(6) (2022) 375-383.
37. Q. Wu, J. Xie, J. Li, Y. Men, F. Yan, Engineering Rapeseed Germination and Root Growth with Mechanical Strength of Polysaccharide Hydrogel, ACS Applied Bio Materials 7(5) (2024) 3496-3505.
38. Z. Teng, Y. Luo, D.J. Pearlstein, B. Zhou, C.M. Johnson, J. Mowery, Q. Wang, J.M. Fonseca, Agarose hydrogel composite supports microgreen cultivation with enhanced porosity and continuous water supply under terrestrial and microgravitational conditions, International journal of biological macromolecules 220 (2022) 135-146.
39. N.J. Amaya-Chantaca, M. Caldera-Villalobos, J.A. Claudio-Rizo, Semi-IPN hydrogels of collagen and gum arabic with antibacterial capacity and controlled release of drugs for potential application in wound healing, 12(1) (2023) 25-40.
40. M. Simon, R. Fulchiron, F. Gouanvé, Water Sorption and Mechanical Properties of Cellulosic Derivative Fibers, Polymers, 2022.
41. L. Gao, H. Luo, Q. Wang, G. Hu, Y. Xiong, Synergistic Effect of Hydrogen Bonds and Chemical Bonds to Construct a Starch-Based Water-Absorbing/Retaining Hydrogel Composite Reinforced with Cellulose and Poly(ethylene glycol), ACS Omega 6(50) (2021) 35039-35049.
42. Saruchi, V. Kumar, H. Mittal, S.M. Alhassan, Biodegradable hydrogels of tragacanth gum polysaccharide to improve water retention capacity of soil and environment-friendly controlled release of agrochemicals, International journal of biological macromolecules 132 (2019) 1252-1261.
43. C. Barrientos-Sanhueza, D. Cargnino-Cisternas, Bacterial Alginate-Based Hydrogel Reduces Hydro-Mechanical Soil-Related Problems in Agriculture Facing Climate Change, 14(5) (2022).
44. Z. Liu, A. Basem, L. Mostafa, D.J. Jasim, A.H. Al-Rubaye, S. Salahshour, M. Hekmatifar, S. Esmaeili, Investigating the effect of pH on the swelling process, mechanical and thermal attributes of polyacrylamide hydrogel structure: A molecular dynamics study, Case Studies in Thermal Engineering 55 (2024) 104148.

45. E.E. Lopéz-Martínez, J.A. Claudio-Rizo, M. Caldera-Villalobos, J.J. Becerra-Rodríguez, D.A. Cabrera-Munguía, L.F. Cano-Salazar, R. Betancourt-Galindo, Hydrogels for Biomedicine Based on Semi-Interpenetrating Polymeric Networks of Collagen/Guar Gum: Applications in Biomedical Field and Biocompatibility, Macromolecular Research 30(6) (2022) 384-390.
46. J.A. Claudio-Rizo, N.G. Hernandez-Hernandez, L.F. Cano-Salazar, T.E. Flores-Guía, F.N. de la Cruz-Durán, D.A. Cabrera-Munguía, J.J. Becerra-Rodríguez, Novel semi-interpenetrated networks based on collagen-polyurethane-polysaccharides in hydrogel state for biomedical applications, Journal of Applied Polymer Science 138(4) (2021) 49739.
47. T.C. Ho, C.C. Chang, H.P. Chan, Hydrogels: Properties and Applications in Biomedicine, 27(9) (2022).
48. J. Xie, M. Bao, S.M.C. Bruekers, W.T.S. Huck, Collagen Gels with Different Fibrillar Microarchitectures Elicit Different Cellular Responses, ACS Applied Materials & Interfaces 9(23) (2017) 19630-19637.
49. Z. Shi, T.-G. Chang, F. Chen, H. Zhao, Q. Song, M. Wang, Y. Wang, Z. Zhou, C. Wang, S.-C. Zhou, B. Wang, G. Chen, X.-G. Zhu, Morphological and physiological factors contributing to early vigor in the elite rice cultivar 9,311, Scientific Reports 10(1) (2020) 14813.
50. B. Akyüz, Effect of different carbon sources and concentrations on in vitro propagation of chestnut, Plant Cell, Tissue and Organ Culture (PCTOC) 160(2) (2025) 25.

Figures

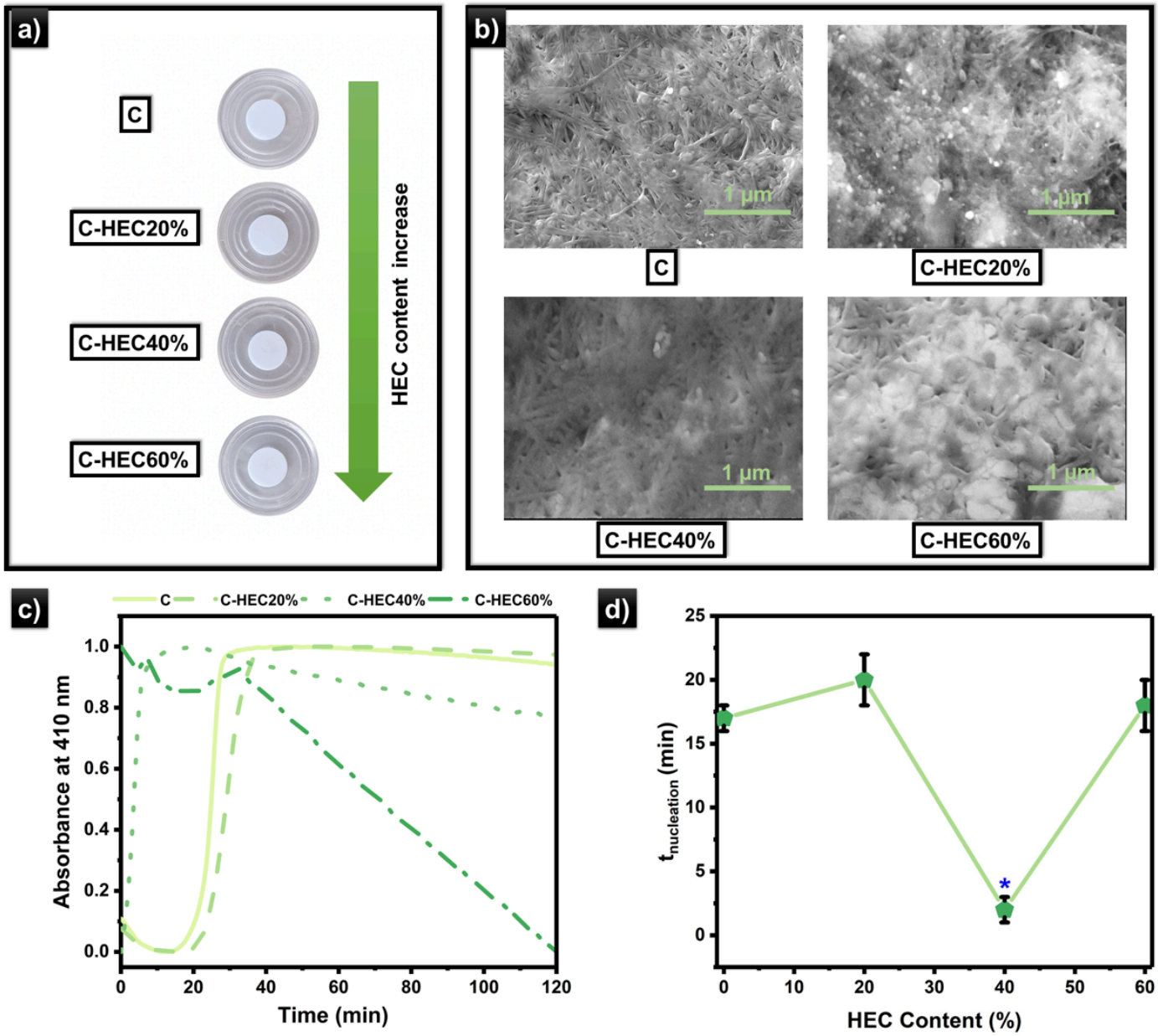

Figure 1

Physical appearance, morphology, and gelation kinetics of collagen–HEC hydrogels. (a) Macroscopic aspect; (b) SEM showing fibrillar structure and HEC granules; (c) Gelation kinetics by turbidity at 410 nm; (d) Nucleation times highlighting rapid gelation in C–HEC40%.

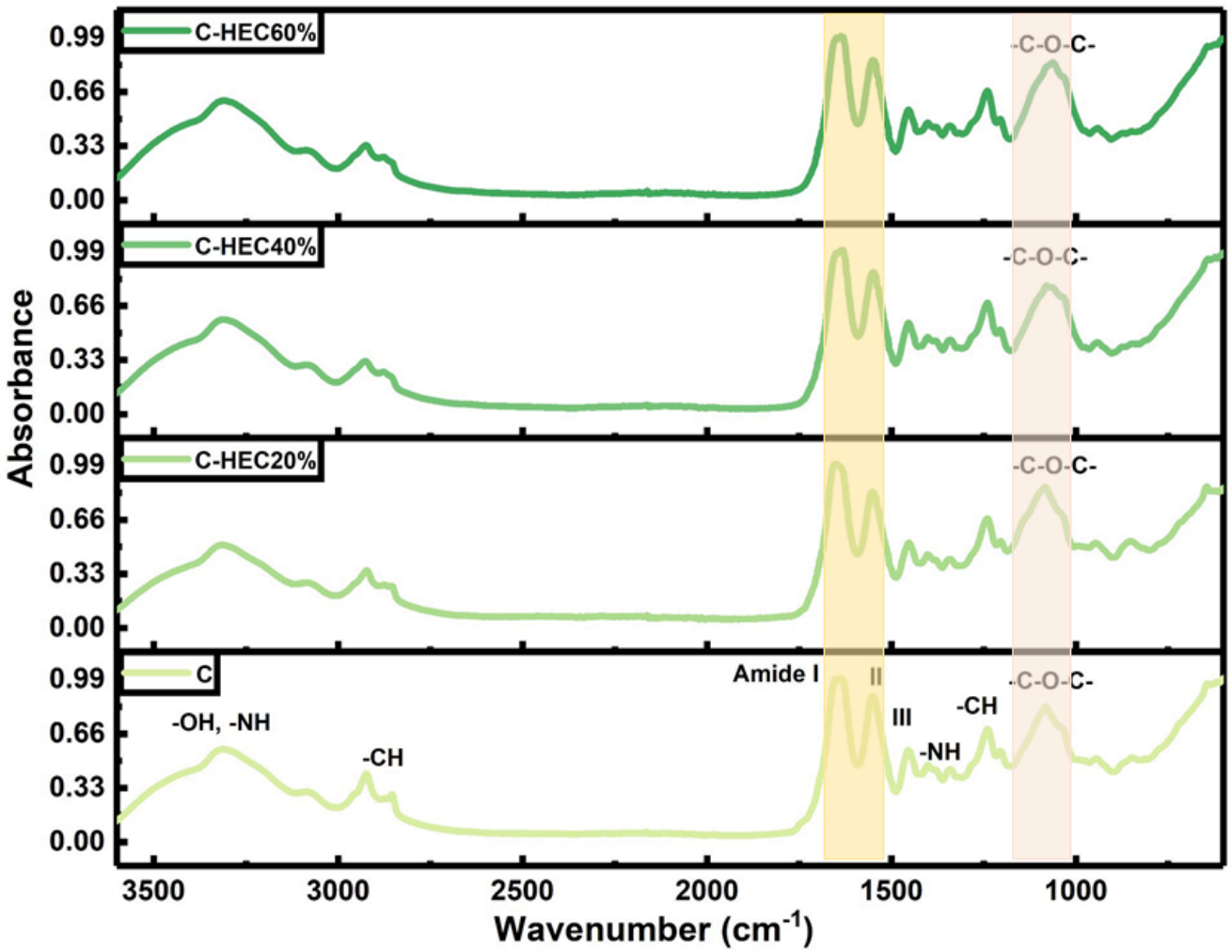

Figure 2

FTIR spectra of collagen–HEC scaffolds showing characteristic functional groups.

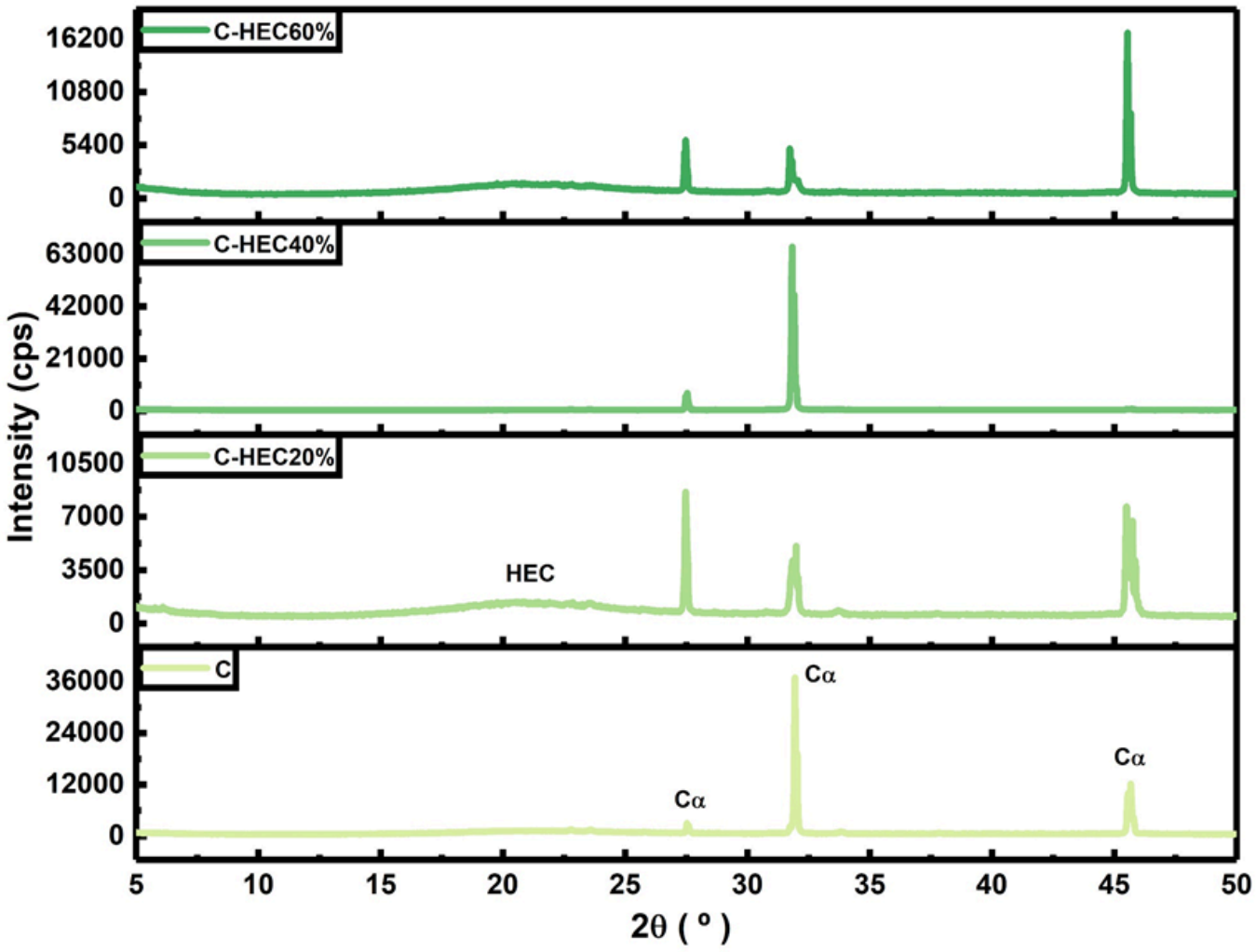

Figure 3

WAXS diffractograms of collagen–HEC scaffolds showing structural transitions with increasing HEC content.

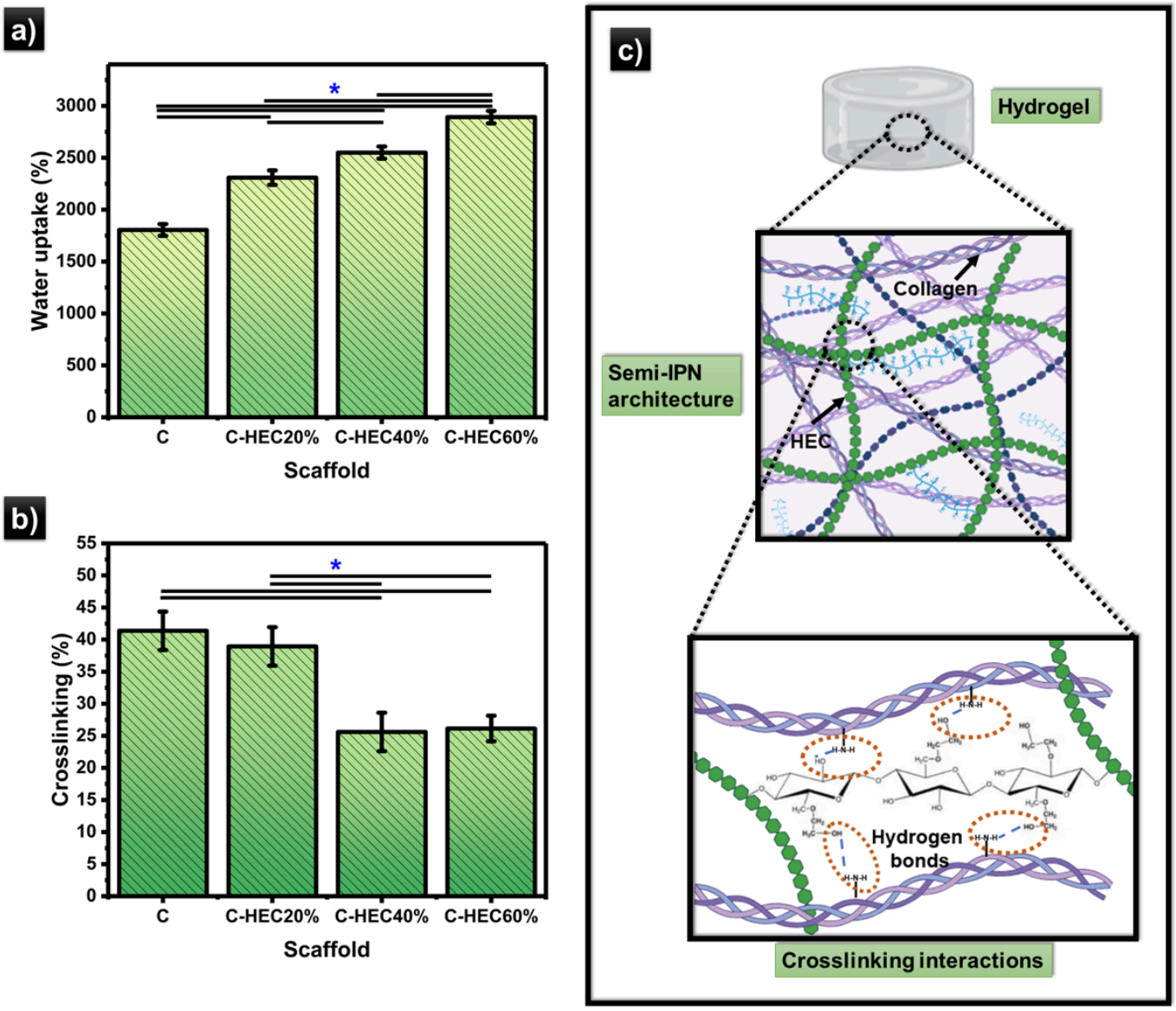

Figure 4

(a) Swelling capacity of collagen–HEC scaffolds. (b) Crosslinking index measured by ninhydrin assay. (c) Illustration of hydrogen bonding stabilizing the semi-IPN structure.

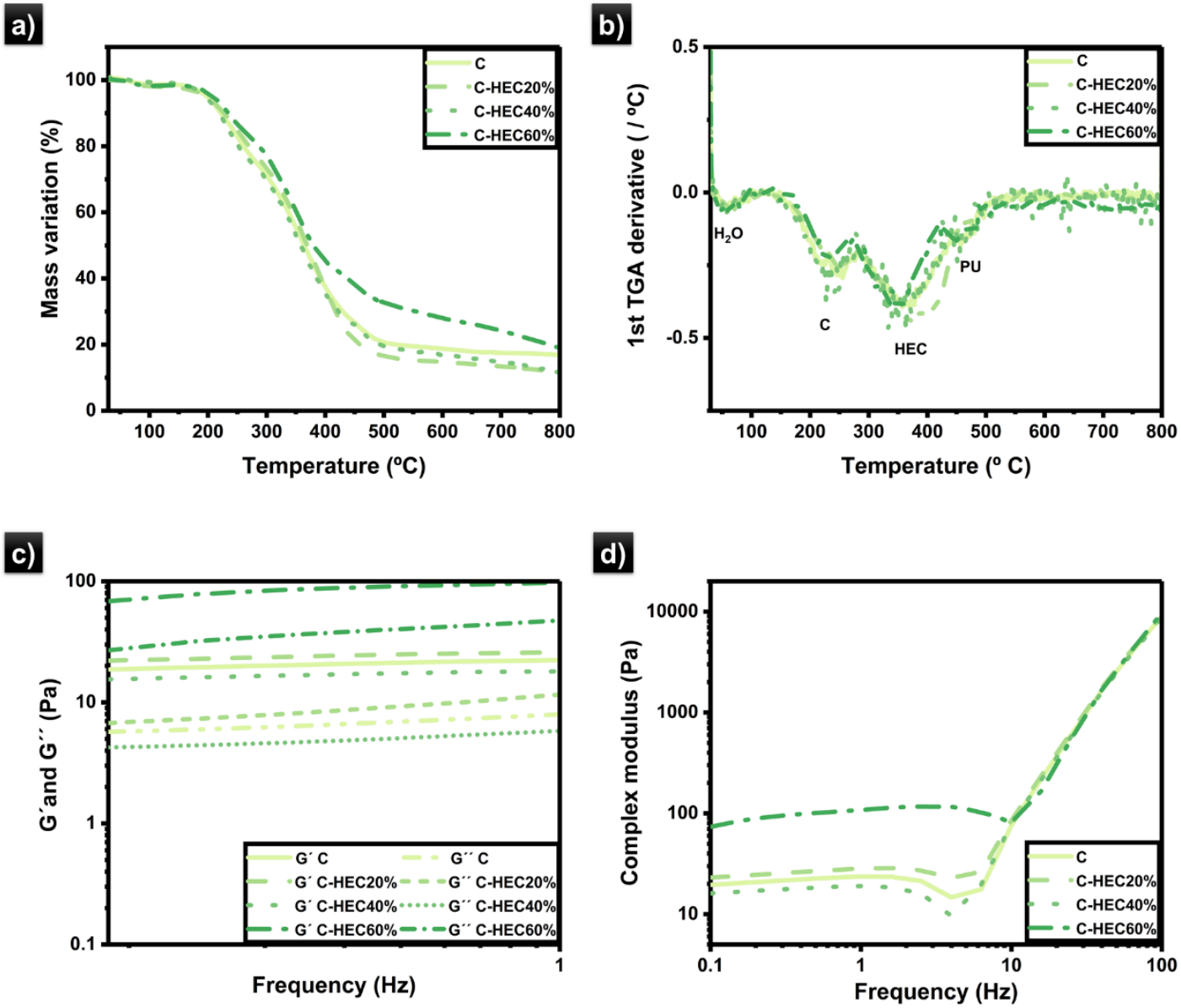

Figure 5

(a) TGA profiles of collagen–HEC scaffolds. (b) First derivative (DTGA) curves showing decomposition events. (c) Storage modulus (G') and complex modulus (G*) indicating viscoelastic behavior and mechanical reinforcement with increasing HEC content.

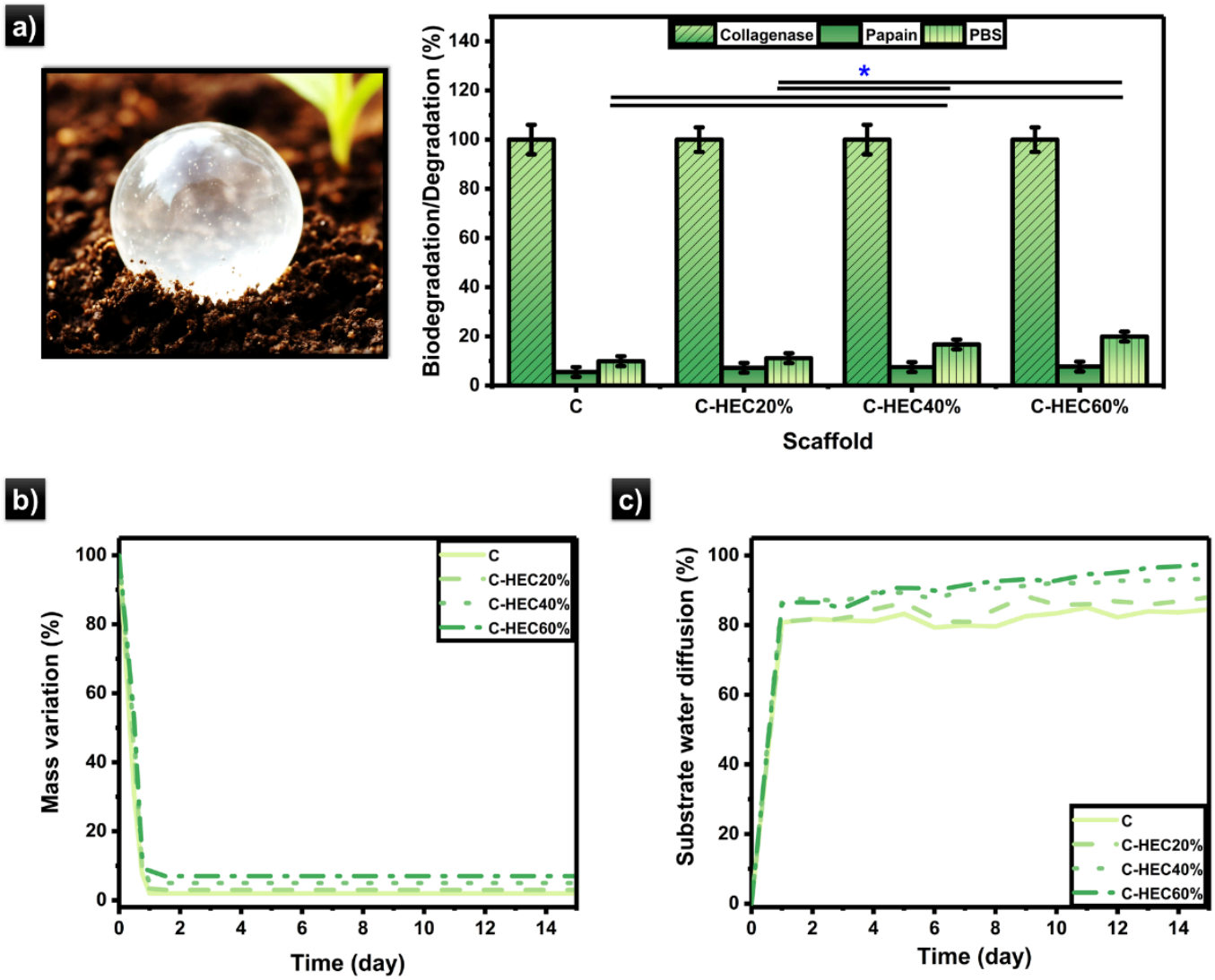

Figure 6

Biodegradation and water diffusion performance of collagen–HEC scaffolds under conditions relevant to agriculture. (a) Mass loss under enzymatic (collagenase, papain (14 U/scaffold)) and hydrolytic (1x PBS) degradation; (b) mass retention in commercial horticultural substrate; (c) water release into substrate over 15 days.

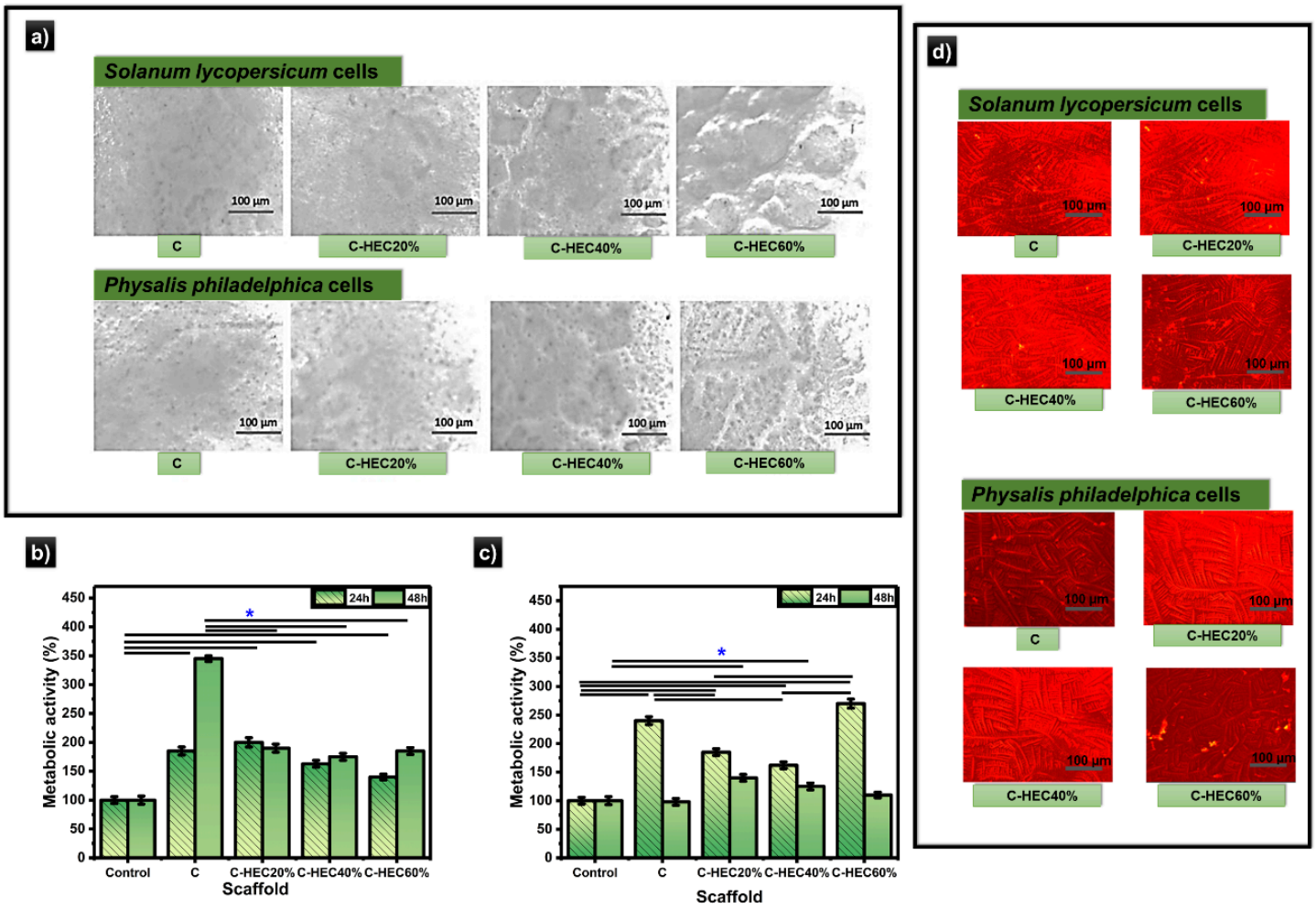

Figure 7

Evaluation of tomato-derived cell behavior on collagen–HEC scaffolds. (a) Microscopic images showing cell adhesion and migration on scaffold surfaces after 48 h. (b) Metabolic activity of red tomato cells at 24 and 48 h assessed by MTT assay. (c) Metabolic activity of green tomato cells at 24 and 48 h. (d) Fluorescence microscopy images showing cell proliferation after 48 h, stained with rhodamine B.

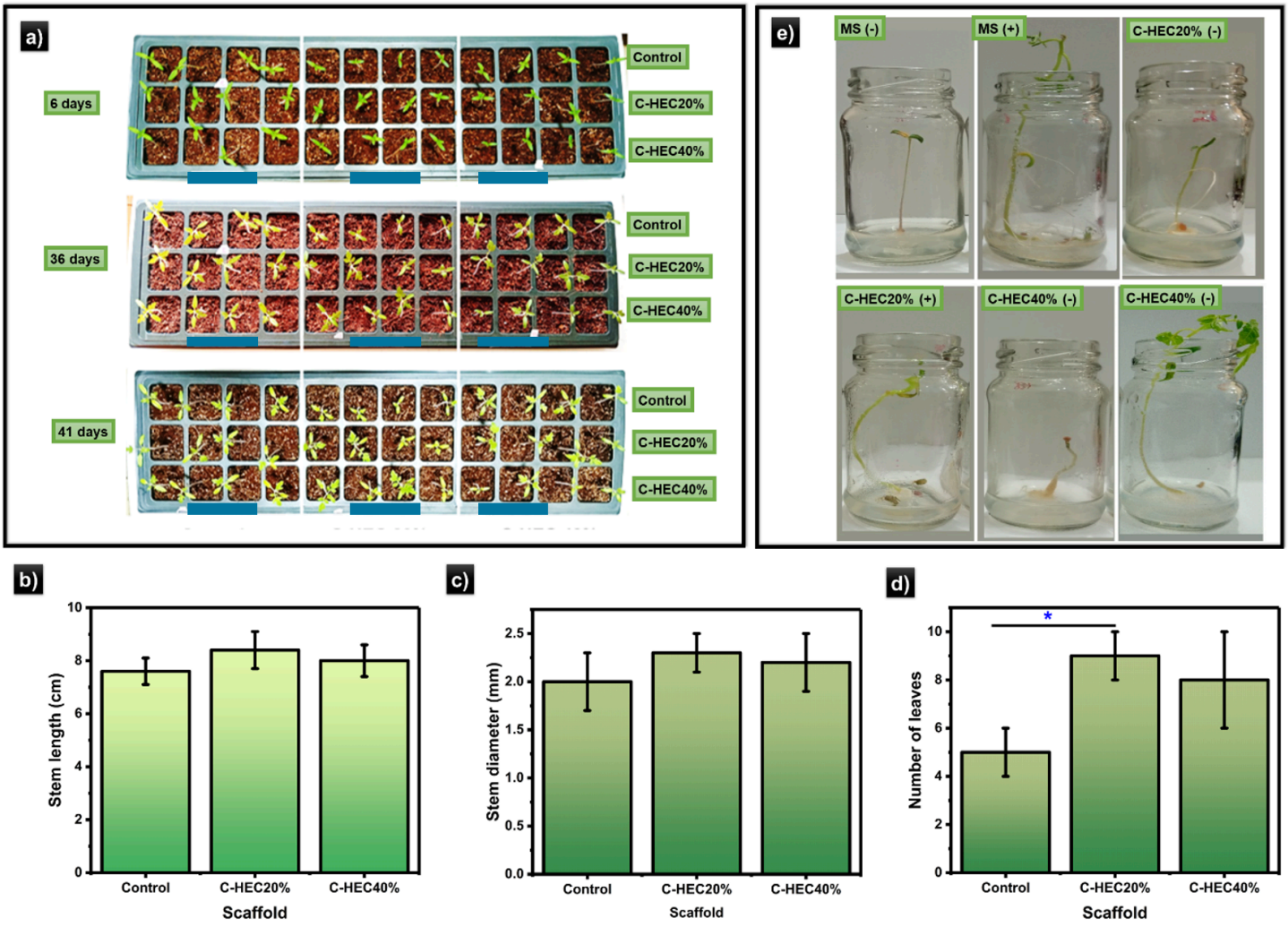

Figure 8

Evaluation of tomato seed germination and plant development over 41 days in commercial vegetable substrate and MS-based *in vitro* systems. (a) Representative images of plant growth. (b–d) Quantification of stem length, stem diameter, and number of leaves. (e) *In vitro*germination on MS agar with or without sucrose and with collagen–HEC hydrogels.

Supplementary Files

This is a list of supplementary files associated with this preprint. Click to download.

- floatimage1.png